

Role of diagonal tension crack in size effect of shear strength of deep beams

Y. Tanaka & T. Shimomura

Nagaoka University of Technology, Niigata, Japan

M. Watanabe

Uchiyama Advance Co. Ltd., Chiba, Japan

ABSTRACT: To clarify the effect of cracking propagation behavior especially on the size effect of deep reinforced concrete beams, 17 deep beams were tested in this study. Experimental factors are specimen size, depth, shear span to effective height ratio (a/d) and bonding of longitudinal bars. 6 beams were un-bonded not to induce diagonal tension crack. As a result, these un-bonded beams had small size effect regardless of a/d while bonded beams showed relatively strong size effect in case of 1.5 of a/d . Because the cracking pattern of diagonal crack influences on the strength of compressive concrete strut, we developed simplified truss model which can deal with the effect of diagonal cracking path on the strength of deep beams and short beams. Proposed model is verified with past researches. As a result, it is clarified that proposed model tends to overestimate the shear strength when bearing failure occurs.

1 INTRODUCTION

The shear strength of reinforced concrete members depends on the compressive strength of concrete, reinforcement ratio, effective depth and span to effective depth ratio (a/d). There exist other factors which influence on the shear capacity especially in deep beams. When deep beams are loaded, the stress around the loading point and the anchorage zone reaches high level compared with slender beams. Therefore, bearing failure or anchorage failure easily occurs prior to shear failure. This premature failure leads to the reduction of load carrying capacity. As to the size effect of deep beams, some researches report that deep beam has strong size effect, while the other researches come to the opposite conclusion. This discrepancy may be caused from the difference in failure mode or unconsidered factor.

Objective of this study is to clarify the mechanism of size effect in deep beam and to determine its reduction rate. In this study, the influence of the location of diagonal tension crack and the area of bearing plate is investigated experimentally. Reflecting test results, we developed the estimation method for shear strength of deep beam. Proposed model is verified by comparing with past test data.

2 EXPERIMENT

2.1 Overview of Experiment

Shear force is transferred by the tied arch system in deep beam. The strength of tied arch system de-

pends on the strength of concrete strut. Therefore it is considered that the propagation of diagonal crack deteriorates the strength of concrete strut. If so, the shear strength and the size effect will be subjected to the propagation behavior of diagonal crack.

In this experiment, reinforcing bar is unbonded not to transfer tensile stress from reinforcing bar to concrete in some specimens. This treatment leads to the absence of diagonal tension crack because tensile stress does not reach cracking stress due to the lack of stress transfer. Size effect of unbond specimens are examined to extract the effect of diagonal crack on size effect. 1.0 and 1.5 of a/d are selected for testing in this study.

2.2 Specimens

Table 1 and 2 show the summary of specimen details and mix proportion of concrete, respectively. Total number of specimens is 17. a/d is selected as 1.0 or 1.5. Test factors are bonding of longitudinal bar, effective depth and the area of bearing plate. Maximum size of aggregate is constant as 25 mm in every specimen. Because the width of smallest specimen is 50 mm, smallest specimens were casted laterally while other specimens were casted vertically. Compressive strength and elastic modulus in Table 1 were measured on the day of beam test.

The ratio between width b and effective depth d of No.1~No.12 specimens is fixed as 0.25 not to fail in bearing failure mode. Cover depth c is defined as

Table 1. Summary of specimen details.

No.	Beam designation	Bond	Effective depth d (mm)	Shear span to depth ratio a/d	Beam width b and Width of bearing plate r (mm)	Loading point	concrete				reinforcing bar		
							Compressive strength f_c (N/mm ²)	Young's modulus E_c (N/mm ²)	Yielding stress f_y (N/mm ²)	Young's modulus E_s (N/mm ²)	Number n	Reinforce cement ratio p_w (%)	Diameter (mm)
No.1	B2-1.0 (50-II)	Yes	200	1.0	50	2	22.6	22100	1360	200000	1	0.64	9.0
No.2	B4-1.0		400		100		29.2	28300	1400	202000	2	0.62	12.6
No.3	B8-1.0		800		200		27.1	27000	1159	200000	1	0.64	36.0
No.4	UB2-1.0	No	200	1.5	50	2	23.2	23400	1360	200000	1	0.64	9.0
No.5	UB4-1.0		400		100		29.2	28300	1400	202000	2	0.62	12.6
No.6	UB8-1.0		800		200		26.6	28600	1159	200000	1	0.64	36.0
No.7	B2-1.5	Yes	200	1.5	50	2	36.8	33300	1360	200000	1	0.64	9.0
No.8	B4-1.5		400		100		33.6	32200	1400	202000	2	0.62	12.6
No.9	B8-1.5		800		200		26.9	29800	1159	200000	1	0.64	36.0
No.10	UB2-1.5	No	200	1.5	50	2	36.8	33300	1360	200000	1	0.64	9.0
No.11	UB4-1.5		400		100		34.9	33500	1400	202000	2	0.62	12.6
No.12	UB8-1.5		800		200		26.7	29800	1159	200000	1	0.64	36.0
No.13	50-I	Yes	200	1.0	50*	1	29.8	31000	1360	200000	1	0.64	9.0
No.14	100-I				100*		29.8	31000	1400	202000	1	0.62	12.6
No.15	200-I				200*		29.6	31400	1400	202000	2	0.62	12.6
No.16	100-II	Yes	200	1.0	100*	2	27.5	26800	1400	202000	1	0.62	12.6
No.17	200-II				200*		28.2	27400	1400	202000	2	0.62	12.6

* Width of bearing plate r is 50 mm in No.13-No.17

Table 2. Mix proportion.

Maximum size of aggregate G_{max} (mm)	Slump (cm)	W/C (%)	Sand percentage s/a (%)	Unit weight (kg/m ³)				
				Water W	Cement C	Sand S	Coarse aggregate G	Additive A_d
25	12.0	59.0	42.5	150	254	798	1132	0.762

Early strength cement, Nominal strength: 18N/mm²

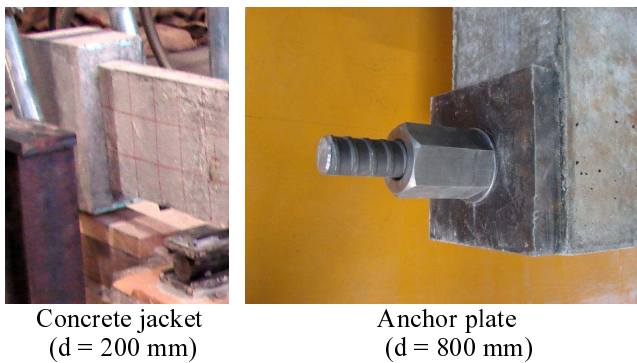


Figure 1. Strengthening in end part.

0.5 times of width b to get similar bond strength regardless of specimen size. To remove bond between concrete and reinforcing bars, boxboard and Teflon sheet were wrapped around the longitudinal bars. Unbonding treatment ranged 0.8 times of loading span.

No.13~No.17 and No.1 specimens were made to examine the influence of bearing stress. Cover depth in these specimens is 25 mm.

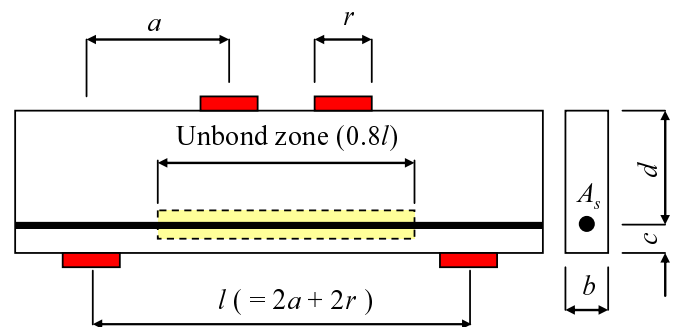


Figure 2. Unbond zone in specimens (2 point loading).

Deformed PC bars which have more than 1100 N/mm² of yielding stresses were utilized not to yield before shear failure occurs.

Reinforcement ratio is about 0.6 % in every specimen. End parts of small and medium specimens (200 mm and 400 mm of effective depth, respectively) were strengthened by concrete jacketing to avoid premature anchorage failure. In large specimens (800 mm of effective depth), anchor plates were provided instead of concrete jacketing.

Table 3. Maximum shear load and the location of diagonal-crack at neutral axis.

No.	Max. shear load V_u (kN)		Location of diagonal crack l_1 (mm)	Bearing stress (N/mm ²)
	Exp.	Cal.		
No.1	48	32	147	19.2
No.2	226	152	313	22.6
No.3	685	580	575	17.1
No.4	45	33	129	17.8
No.5	217	152	345	21.7
No.6	668	573	647	16.7
No.7	36	27	251*	14.3
No.8	114	103	538	11.4
No.9	258	355	991	6.4
No.10	41	27	300*	16.3
No.11	173	105	600*	17.3
No.12	444	353	1294	11.1
No.13	45	39	134	36.0
No.14	90	77	166	35.8
No.15	174	153	163	34.9
No.16	95	73	151	19.0
No.17	189	148	158	18.9

*Estimation, diagonal crack did not occur

2.3 Test Method

Simply supported beam specimens were loaded under two point loadings. Loading is conducted statically until failure. The ratio of the width of bearing plate r to the effective depth d is kept as 0.25 not to change bearing stress around loading and supporting points. Load, center deflection and crack patterns are measured during the test.

2.4 Test Results

Maximum shear force and the location of diagonal crack are summarized in Table 3. Maximum shear force in Table 3 equals the half of maximum load in experiment. Specimens were failed in shear except No.7, No.10 and No.11.

Crack patterns of bonded and unbonded specimens are compared in Figure 13 and Figure 14. Regardless of a/d , only one flexural crack was induced in unbonded specimens. This is because tensile stress cannot be transferred after first crack is induced in unbonded specimens.

The location of diagonal crack shifts on the inside when bond is removed (see Figure 13, 14 and Table 3). In case of bonded specimens, concrete strut is degraded due to the diagonal crack. On the other hand, concrete strut in unbonded specimen is sound

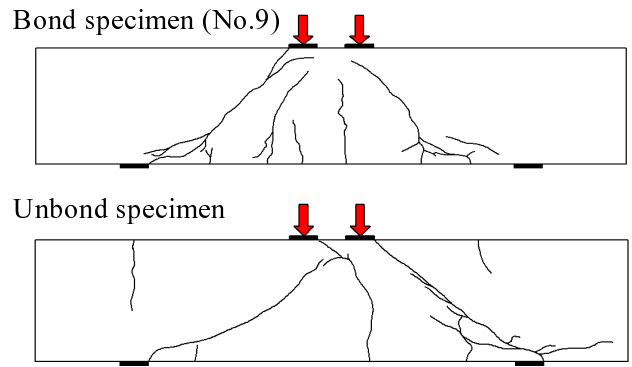


Figure 3. Crack pattern ($d = 800$ mm, $a/d = 1.0$).

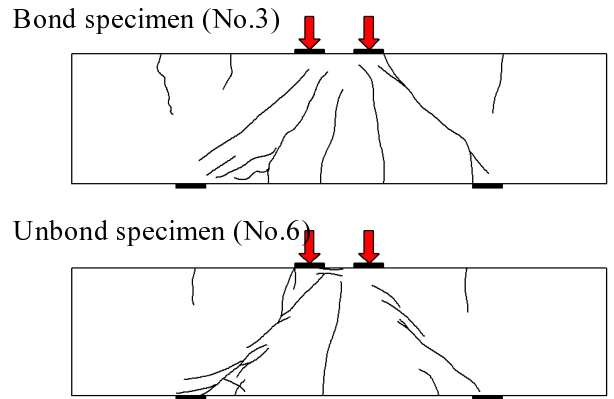


Figure 4. Crack pattern ($d = 800$ mm, $a/d = 1.5$).

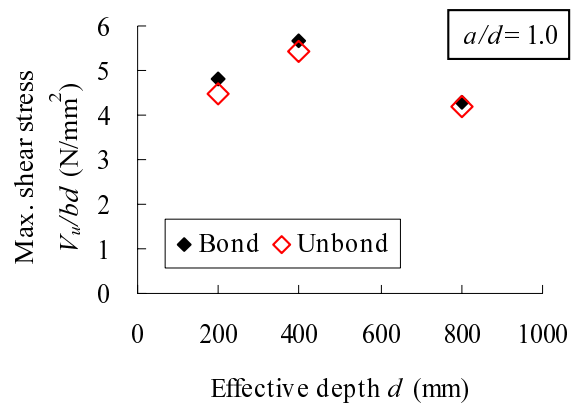


Figure 5. Relationship between maximum shear stress and effective depth (No.1~No.6).

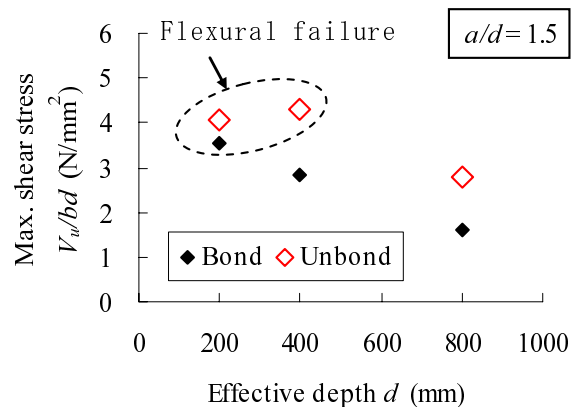


Figure 6. Relationship between maximum shear stress and effective depth (No.7~No.12).

owing to the shift of diagonal crack. Question is why the location of diagonal crack is shifted. The answer will be the process of diagonal crack. In No.9, diagonal crack originates from the tip of flexural crack while diagonal crack occurred apart from flexural crack in No.6 and No.12.

The diagrams in Figure 5 and Figure 6 indicate the size effect of deep beams in case of 1.0 and 1.5 of a/d , respectively. Vertical axis is nominal shear strength in these figures. When a/d is 1.5, shear strength of unbonded specimens are higher than that of bonded specimens. On the other hand, shear strength of unbonded member is same with that of bonded specimens in case of 1.0 of a/d .

Because compressive strength of concrete showed a wide range, test results are modified to remove the effect of compressive strength. In Figure 7 and 8, test results are converted to relative strength. relative strength is defined as the ratio of test result to the estimated strength. Detail of estimation method is described in latter part of this paper. In the estimation method, the location of diagonal crack l_1 is required. In estimation, test data shown in Table 3 is used for l_1 . Diagonal crack did not occur in several specimens which failed in flexural. In such case, the location of diagonal crack is assumed from equation 8 for bonded specimen while $l_1 = a$ is assumed for unbonded specimens.

Size effect in deep beam ($a/d = 1.0$) is relatively small both in bond and unbond specimens as shown in Figure 7.

Similar results have been reported by some researchers (Zhang & Tan, 2007) while other researches have been reported significant size effect in deep RC beams (Walraven & Lehwalter 1994; Yang et al. 2003). Authors believe the discrepancy in these researches is mainly caused by the difference in failure mode. Width and length of bearing plate is proportional in former researches while width or length of bearing plate is constant in latter researches. Therefore, bearing failure tends to occur in latter researches especially in large specimen. Size effect of deep beam will be small when bearing failure and anchorage failure are avoided in deep beam.

Size effect in short beam which has 1.5 of a/d is indicated in Figure 8. Bonded specimens have relatively strong size effect compared with unbonded specimens. However, the number of test data is not sufficient because some of them did not fail in shear.

Therefore, test data of short beams ($a/d = 1.5$) are collected from past researches (Kousa et al. 2007; Kobayashi et al. 2005; Moody et al. 1954) and compared with test results of this study. Effective depth of collected data ranges 400~1400 mm. Test data of 39 deep beams are indicated in Figure 9. To remove the effect of concrete strength, test results are normalized by evaluated shear strength which is calculated by equation 1~9. Regression curve for past research is

also indicated in this figure. The regression curve verified that shear strength decreases directly with the $-1/3$ power of effective depth when a/d is 1.5.

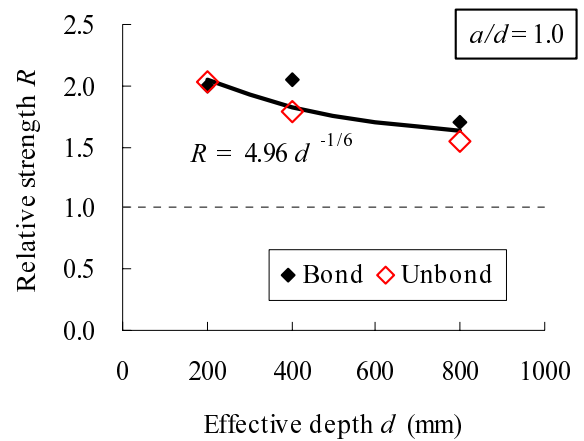


Figure 7. Relationship between relative strength and effective depth (No.1~No.6).

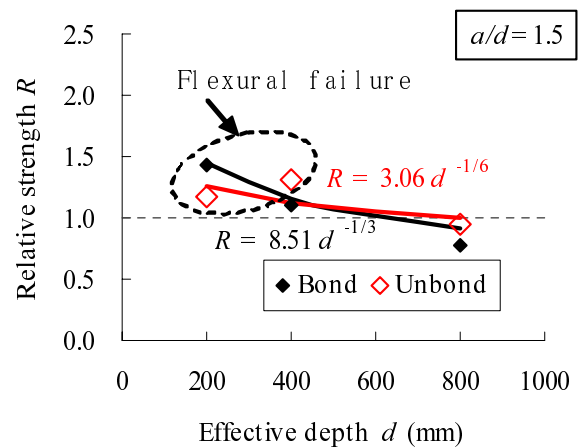


Figure 8. Relationship between relative strength and effective depth (No.7~No.12).

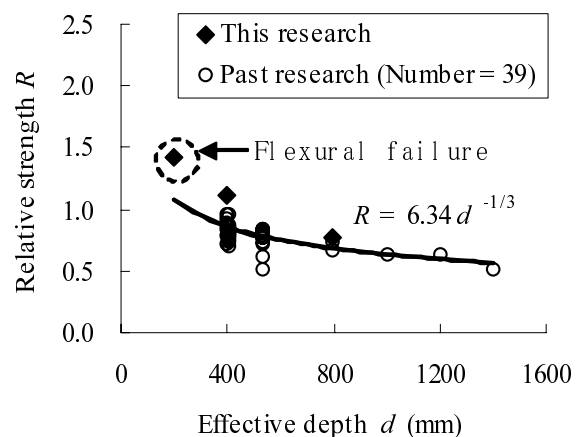


Figure 9. Comparison between this research and past research ($a/d = 1.5$).

Maximum bearing stress is summarized with regard to the width of deep beams which have 200 mm of effective depth in Figure 10 and 11. Figure 10 is for one point loading while Figure 11 is for two points

loading. Diagonal cracking stress and axial compressive strength are indicated in these figures. Maximum bearing stress is 20 % larger than compressive strength in case of one point loading as shown in Figure 10. These specimens failed when diagonal crack occurred. Width of specimen does not effect on the shear strength of deep beam in this case.

Maximum bearing stress is less than compressive strength in case of two points loading as shown in Figure 11. Failure load is larger than diagonal cracking load when width of specimen is larger than 100 mm. The propagation of diagonal crack may be restrained when bearing stress is small. If this assumption is true, the degree of size effect will be reduced by reducing bearing stress around loading point. On the other hand, diagonal cracking load does not depend on the width of specimen as reported by past research (Kani 1967). Diagonal cracking load of two points loading is slightly higher than that of one point loading.

The location of diagonal crack is summarized in Figure 12. The distance of diagonal crack from support is measured at neutral axis. a/d and effective depth of these 6 specimens are constant. The variation of the crack location is smaller than maximum aggregate size (25 mm). It is clear that the reproducibility of cracking path is closely related to the size of aggregate.

3 EVALUATION METHOD FOR SHEAR STRENGTH OF DEEP BEAM

3.1 Truss Arch Model

Authors have been proposed truss arch model to evaluate the shear strength of deep RC beams (Tanaka et al. 2005). In this model, outside of diagonal crack is assumed as compressive strut while longitudinal bars are assumed as tension tie. When point load is applied to RC deep beams as illustrated in Figure 13, shear strength is evaluated by following equation which is derived from equilibrium of force in truss system.

$$V_{cdd} = k_1 \cdot \beta \cdot f'_c \cdot b \cdot Z'_c \cdot \left(1 + (a/d)^2\right)^{-0.5} \quad (1)$$

k_1 is the reduction rate of compressive strength f'_c (N/mm^2). This reduction rate is estimated from Equation 2 which is defined based on Collins model (Collins et al. 1993).

$$k_1 = \begin{cases} 1.0 & (f'_c \leq 25) \\ 0.6 + \frac{10}{f'_c} & (f'_c > 25) \end{cases} \quad (2)$$

β is the coefficient of equivalent stress block estimated from following equation.

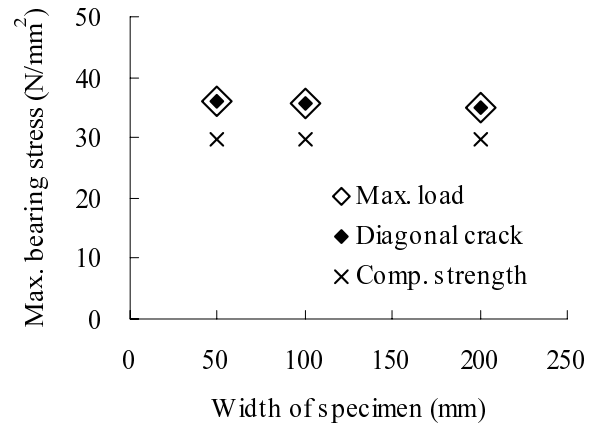


Figure 10. Effect of specimen width on maximum shear stress (1 point loading).

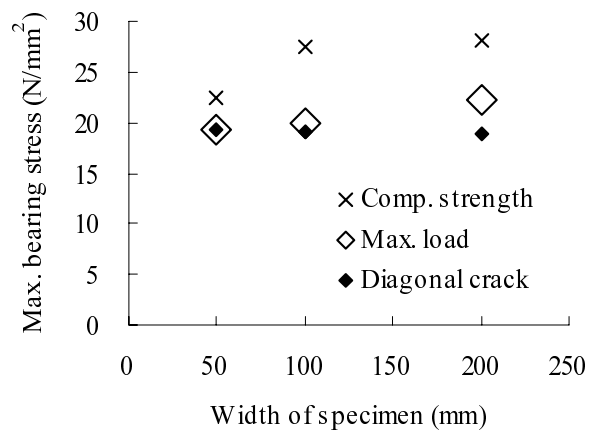


Figure 11. Effect of specimen width on maximum shear stress (2 point loading).

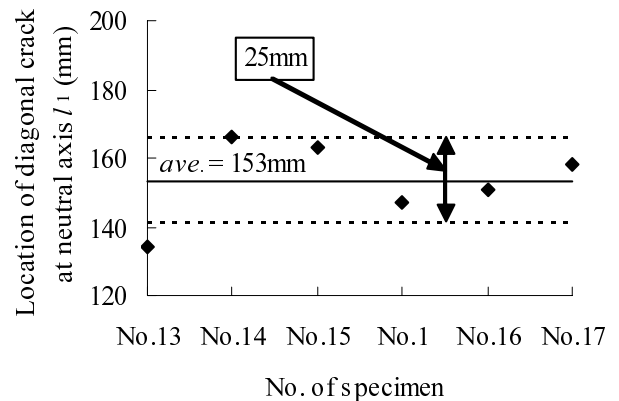


Figure 12. Distance between diagonal crack and support at neutral axis.

$$\beta = 0.52 + 80 \cdot \varepsilon'_{cu} \quad (3)$$

where, ε'_{cu} is peak strain of concrete.

$$\varepsilon'_{cu} = \frac{155 - f'_c}{30000} \leq 0.0035 \quad (4)$$

Z'_c used in Equation 1 is the width of arch rib and defined as follows.

$$Z'_c = Z' - z(a) \quad (5)$$

where, Z' is the height of neutral axis in cracked reinforced concrete. $z(a)$ is the distance between diagonal crack and neutral axis at $x = a$. Height of neutral axis is achieved from following equation in which elasticity is assumed for compressive stress of concrete.

$$Z' = p_w \cdot n_s \cdot d \cdot \left(-1 + \sqrt{1 + 2/(n_s \cdot p_w)}\right) \quad (6)$$

where, p_w is effective reinforcement ratio, d is effective depth and n_s is modulus ratio between rebar and concrete.

It is assumed that diagonal crack propagates normal to the direction of principal stress. In such a case, height of diagonal crack is evaluated as follows.

$$z(x) = \int_{l_1}^x \tan \theta \, dx \quad (7)$$

where, l_1 is the distance of diagonal crack from support at neutral axis. In case of point loading, l_1 is estimated from Equation 8 which is defined from collected test data.

$$l_1 = \begin{cases} (1 - 0.11 \cdot a/d) \cdot a & (a/d < 2.7) \\ 0.7 \cdot a & (a/d \geq 2.7) \end{cases} \quad (8)$$

θ in Equation 7 is the direction of diagonal crack. As a result, following relationship is achieved by assuming Elasticity and Bernoulli-Euler theory.

$$\tan 2\theta = \frac{Z'^2 - z(x)^2}{x \cdot z(x)} \quad (9)$$

By solving Equation 5~9 numerically, width of arch rib Z'_c is obtained in this model.

3.2 Modification of Truss Arch Model

Because above mentioned model cannot deal with size effect, coefficient for size effect is required. Referring the regression curve in Figure 7 and 8, coefficient β_d is defined as follows.

$$\beta_d = \begin{cases} (d/200)^{-1/6} & (a/d \leq 1.0) \\ (d/200)^{-1/3} & (a/d > 1.0) \end{cases} \quad (d: \text{mm}) \quad (10)$$

Proposed model tends to underestimate the shear capacity especially in case a/d is small as shown in Figure 14. There will be two causes for the discrepancy. The first is crack propagation. In the proposal model, diagonal crack is assumed to propagate up to loading point at once. However, crack propagation is slow in deep beams due to the re-distribution of stress

after cracking. The second is stress distribution in concrete strut. Because flexural-compression condition is assumed in proposed model, equivalent stress block is

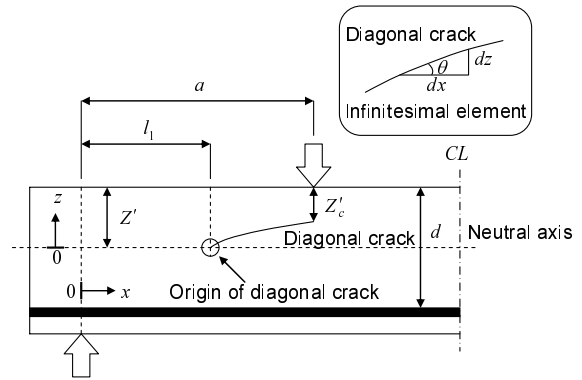


Figure 13. Definition of variables in the estimation of shear strength.

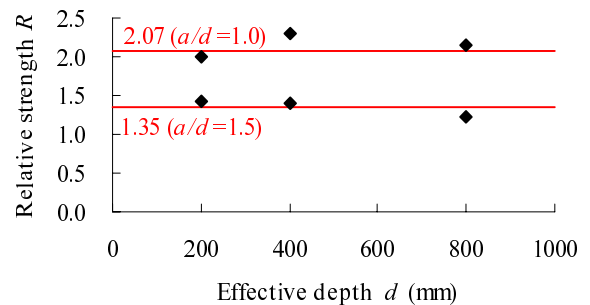


Figure 14. Relative strength of bonded specimens (Equation 10 is applied for size effect).

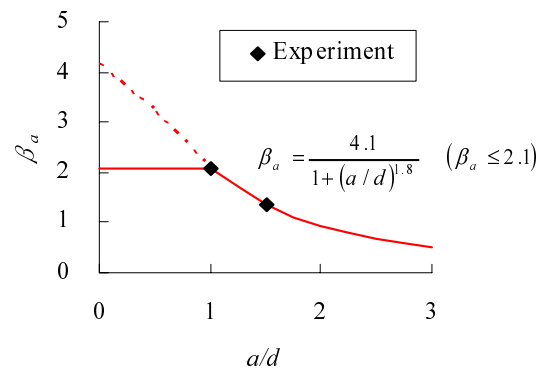


Figure 15. Modification coefficient β_a which deals with the effect of a/d .

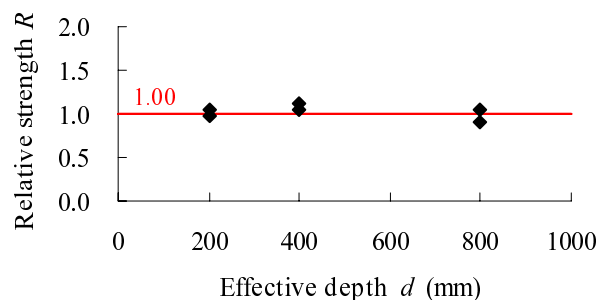


Figure 16. Relative strength of bonded specimens (Equation 12 is applied for estimation).

used to estimate compressive strength of concrete strut. This assumption is appropriate for short or slender beam. On the other hand, stress condition of concrete strut in deep beam is thought to be similar to the axial compression. For these reasons, we decided to use additional coefficient β_a with regard to a/d .

$$\beta_a = \frac{4.1}{1+(a/d)^{1.8}} \quad (\beta_a \leq 2.1) \quad (11)$$

This equation is defined to match test results in this study (see Fig. 15). Upper limit is decided as 2.1 ($a/d = 1$) because we do not have test data which is less than 1 in a/d .

As a result, equation for shear strength is modified as shown in Equation 12.

$$V_{cdd} = k_1 \cdot \beta \cdot \beta_a \cdot \beta_d \cdot f'_c \cdot b \cdot Z'_c \cdot (1+(a/d)^2)^{0.5} \quad (12)$$

This equation covers 1.0~2.0 regarding a/d .

Estimated shear strength are compared with test results in Figure 16. It is clear that truss arch model is modified to match test results in this study.

3.3 Bearing failure load

Truss arch model can estimate the failure load when diagonal concrete strut fails in shear compression. However, this model cannot deal with bearing failure which occurs around bearing plate because assumed failure mode is different. When deep beam fails in bearing failure mode, another estimation method is required.

In this study, it is assumed that bearing failure occurs when bearing stress reaches bearing strength. Following the assumption, bearing failure load is obtained from Equation 13.

$$V_b = \frac{1}{2} \cdot k \cdot n \cdot f'_c \cdot b \cdot r \quad (13)$$

where n is the number of loading point (1 or 2), r is the width of bearing plate and k is the ratio of bearing strength to compressive strength. Referring to Figure 10, k is assumed as 1.2. In Equation 13, perfect bearing condition is assumed. However, past research pointed out premature failure may occur when the contact between bearing plate and concrete is not smooth (Kousa et al. 2006).

3.4 Yielding Load

Shear force at yielding is evaluated from Equation 14. This equation is derived from equilibrium of force in truss analogy.

$$V_y = \frac{A_s \cdot f_y}{a/d} \quad (14)$$

3.5 Verification of Proposed Model

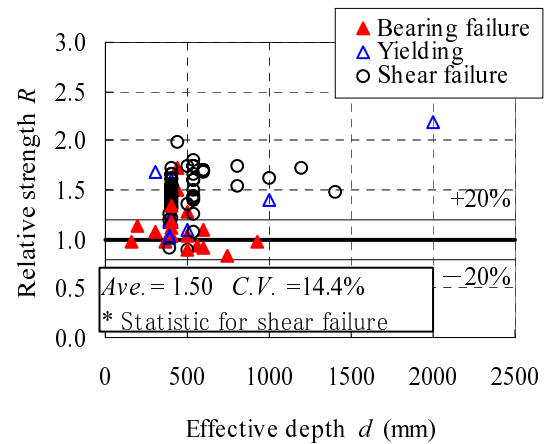


Figure 17. Comparison between test results and JSCE equation.

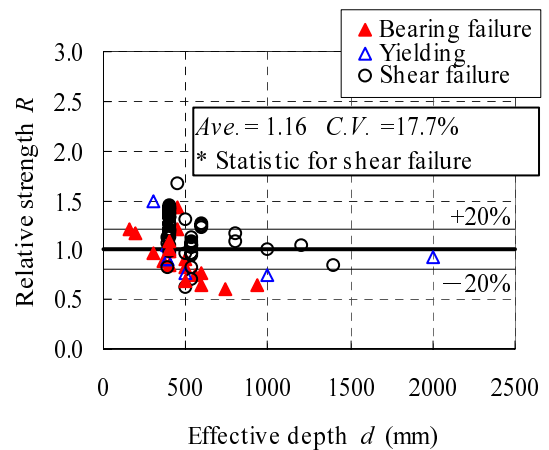


Figure 18. Comparison between test results and Niwa's equation.

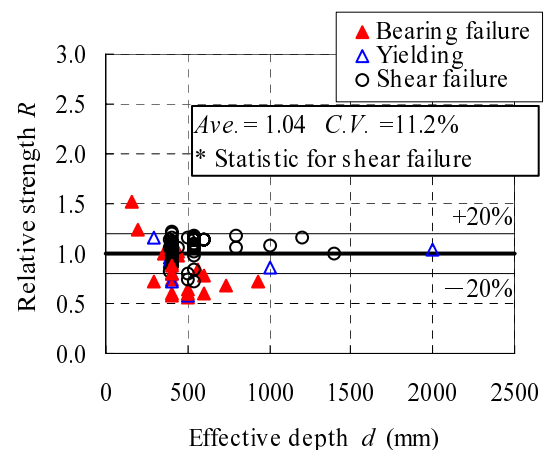


Figure 19. Comparison between test results and proposed model.

Modified truss arch model is verified with test data in past researches (Moody et al. 1954; Mathey & Watstein 1963; Clark 1951; Tan & Lu 1999; Oh & Shin 2001). Every specimen does not have shear reinforcement. The ranges of related factors of collected test data are indicated in Table 4.

Table 4. Ranges of experiments both in this research and past researches.

		Experiment in this research used to develop the estimation method	Experiment in past research used for verification (Total number = 81)
Effective depth	d	200~800mm	160~2000mm
Comp. Strength of concrete	f'_c	22.6~36.8N/mm ²	17.2~123N/mm ²
Reinforcement ratio	p_w	0.6%	0.27~4.25%
Ratio of loading width to effective depth	r/d	0.25	0.22~0.38
Ratio of specimen width to effective depth	b/d	0.25	0.20~1.56
Shear span to effective depth ratio	a/d	1.0 or 1.5	0.5 ~ 2.0

Strength of deep and short beams is estimated as the minimum value between equation 12-14. Shear strength of test specimen is estimated with JSCE equation and Niwa's equation to compare with proposed model.

JSCE equation is as follows.

$$V_{cdd} = \beta_d \cdot \beta_p \cdot \beta_a \cdot f_{dd} \cdot b \cdot d / \gamma_b \quad (16)$$

where, $\beta_d = \sqrt[4]{1000/d}$ (d : mm) but $\beta_d \leq 1.5$,

$$\beta_p = \sqrt[3]{p_w/100} \quad \text{but} \quad \beta_p \leq 1.5,$$

$$\beta_a = \frac{5}{1 + (a_v/d)^2}, \quad a_v = a - \frac{r}{2},$$

$$f_{dd} = 0.19 \cdot \sqrt{f'_c}, \quad \gamma_b = 1.0 \quad \text{in this study.}$$

On the other hand, Niwa's equation is as follows.

$$V_{cdd} = 0.244 \times \frac{f'_c{}^2 \cdot (1 + \sqrt{p_w}) \cdot \{1 + 3.33 \cdot (r/d)\}}{1 + (a/d)^2} \cdot b \cdot d \quad (17)$$

Evaluated strength is compared with test results in Figure 17-19. Shear strength in these figures is evaluated by using JSCE equation, Niwa's equation and proposed model, respectively.

Test data is classified according to failure mode in these figures. Test specimens are classified to "bearing failure" if failure mode is written as bearing failure in reference literature or if failure mode is expected as bearing failure by proposed model. Test specimens are classified to "yielding" if failure load is higher than yielding load while other specimens are classified to "shear failure".

JSCE equation is used for the estimation in Figure 17. Average relative strength of JSCE equation is higher than that of others. However, shear strength is evaluated safely regardless of failure mode. This feature is essential for design equation.

Average relative strength of Niwa's equation and proposed model is close to 1.0 compared with JSCE equation as shown in Figure 18-19. In these cases,

shear strength tends to be overestimated if failure mode is estimated as bearing failure.

Bearing failure is sensitive to heterogeneity and stress condition. Therefore, bearing failure can occur when bearing stress is less than axial compressive strength. To improve proposed model, Equation 13 should be modified in future.

4 CONCLUSIONS

In this study, loading test of RC deep beams was conducted. The effect of a/d , effective depth and bond of rebar are examined in the test. Based on the test results, estimation method of shear strength is proposed and verified. As a result, following conclusions are made.

1. Size effect of shear strength is small when a/d is less than 1.0 or when rebar is unbonded on the condition that bearing failure is avoided.

2. There is possibility that size effect is reduced when bearing stress is less than compressive strength. This is because the propagation of diagonal crack is prevented in such a case.

3. The location of diagonal crack has about 25 mm of variation. The value corresponds to maximum size of aggregate.

4. Proposed model is verified when a/d ranges 1 to 2. However, proposed model tends to overestimate the strength of deep beams when bearing failure occurs.

REFERENCES

- Clark, A. P. 1951, Diagonal tension in reinforced concrete beams, ACI journal proceedings, 48, No.2, 145-156.
- Collins, M. P., Mitchell, D. & MacGregor, J. G. 1993, Structural design considerations for high strength concrete, Concrete international, 15, No.13, 27-34.
- Ikeda, N. & Uji, K. 1980. Studies on the effect of bond on the shear behavior of reinforced concrete beams, Proc. JSCE, J. materials, concrete structures and pavements, No.293, 101-109.
- Johnson, H.L. 1965. Artistic development in autistic children. *Child Development* 65(1): 13-16.
- Kani, G. N.J. 1967, How safe are our large reinforced concrete beams?, ACI journal proceedings, 64, No.3, 128-141.

- Kobayashi, H., Unjoh, S. & Salamy, M. R. 2005, Experimental study on shear capacity of large scaled deep beams, Proc. of JCI, 27, No.2, 829-834.
- Kousa, K., Wakiyama, T., Nishioka, T. & Kobayashi, H. 2007, Effect of shear span ratio on the fracture of deep beams, Proc. JSCE, J. materials, concrete structures and pavements, 62, No.4, 798-814.
- Mathey, R. G. & Watstein, D. 1963, Shear strength of beams without web reinforcement containing deformed bars of different yield strength, ACI journal proceedings, 60, No.2, 183-207.
- Moody, K. G., Viest, I. M., Elstner, R. C. & Hognestad, E. 1954, Shear strength of reinforced concrete beams Part 1 – Tests of simple beams, ACI journal proceedings, 26, No.4, 317-332.
- Oh, J. K. & Shin, S. W. 2001, Shear strength of reinforced high strength concrete deep beams, ACI structural journal, 98, No.2, 164-173.
- Tanaka, Y., Kishi, T. & Maekawa, K. 2005, Tied arch system and evaluation method of shear strength of RC members containing artificial crack or unbonded zone, Proc. JSCE, J. materials, concrete structures and pavements, No.788, 175-193.
- Tang, K. H. & Lu, H. Y. 1999, Shear behavior of large reinforced concrete deep beams and code comparisons, ACI structural journal, 96, No.5, 836-845.
- Uchibori, H., Mutsuyoshi, H., Pandey, G. R. & Tanino, R. 2004, Investigation on the shear behavior of reinforced concrete beams with bond controlled reinforcement, Proc. of JCI, 26, No.2, 1027-1032.
- Umemoto, Y., Kousa, K., Kobayashi, H. & Nishioka, T. 2005, Experimental study of deep beams, parameter effect depth, Proc. of JCI, 27, No.2, 823-828.
- Walraven, J. and Lehwalter, N. 1994. Size effects in short beams loaded in shear, ACI structural journal, 91, No.5, 585-593.
- Yang, K. H., Chung, H. S., Lee, E. T. & Eun, H. C. 2003, Shear characteristics of high strength concrete deep beams without shear reinforcements, Engineering structures, 25, 1343-1352.
- Zhang, N. & Tan, K. H. 2007. Size effect in RC deep beams: Experimental investigation and STM verification: Engineering structures, 29, 3241-3254.